The Peculiar Spectral Properties of Amino-Substituted Uracils: A Combined Theoretical and Experimental Study

Ákos Bányász,[†] Szilvia Karpati,[†,‡] Yannick Mercier,[§] Mar Reguero,[§] Thomas Gustavsson,[†] Dimitra Markovitsi,[†] and Roberto Improta*[,†,||]

Laboratoire Francis Perrin, CEA/DSM/IRAMIS/SPAM - CNRS URA 2453, 91191 Gif-sur-Yvette, France, Departament de Química Física i Inorgànica, Universitat Rovira i Virgili, Marcel·lí Domingo, s/n-Campus Sescelades, 43007 Tarragona, Spain, and Istituto Biostrutture e Bioimmagini-CNR, Via Mezzocannone 16, I-80134 Napoli, Italy

Received: June 8, 2010; Revised Manuscript Received: July 22, 2010

A detailed experimental and computational study of the absorption and fluorescence spectra of 5-aminouracil (5 AU) and 6-aminouracil (6 AU) in aqueous solution is reported. The lowest energy band of the steady-state absorption spectra of 5 AU is considerably red-shifted, noticeably less intense, and broader than its counterpart in uracil (U). On the contrary, the 6 AU lowest energy absorption peak is close in energy to that of U, but it is much narrower and the transition is much more intense. The emission properties of 5 AU, 6 AU, and U are also very different. Both amino-substituted compounds exhibit indeed a much larger Stokes shift as compared to U, and the emission band of 5 AU is much narrower than that of 6 AU. Those features are fully rationalized with the help of PCM/TD-PBE0 calculations in aqueous solution and MS-CASPT2/CASSCF calculations in the gas phase. A stable minimum on the potential energy surface of the lowest energy bright state is found for 5 AU, both in the gas phase and in aqueous solution. For 6 AU a barrierless path leads to the conical intersection with the ground electronic state, but a nonplanar plateau region is predicted in aqueous solution, which is responsible for the very large Stokes shift. Some general considerations on the excited-state dynamics of uracil derivatives are also reported.

Introduction

The excited-state behavior of the DNA and its building blocks (the nucleobases) is likely one of the hottest topics in the field of photochemistry and photophysics.[1−6] In fact, besides its intrinsic biological interest, related to the potentially dangerous implications of UV absorption by DNA,[7−9] the large number of accurate experimental and computational studies (too many to be exhaustively cited here) has provided a huge amount of information on the most significant effects ruling the excited-state decay of complex systems (see refs 1−4 and 10−57 and the references therein). Concerning the isolated nucleobases, time-resolved experiments have shown that the lowest energy bright excited states of purines (guanine, adenine) and pyrimidines (uracil, thymine, and cytosine) decay on the subpicosecond timescale.[1−4,11−28] In parallel, calculations have shown that, for all the nucleobases, barrierless paths exist on the lowest energy bright excited state, connecting the Franck−Condon (FC) region with a conical intersection (CI) with the ground electronic state (S_0), thus accounting for their very short lifetimes.[29−57] As a consequence, the excited-state dynamics of isolated nucleobases has been considered well assessed.[1,2] However, the most recent studies, though qualitatively confirming the above picture, have revealed new interesting features, such as the possible involvement of dark excited states in the decay mechanism,[11,12,14,34] or the existence of a broad plateau on the excited-state potential energy surface (PES).[28] Such features still await their definitive assessments. Furthermore, several mechanistic aspects of the nucleobase excited-state decay are still the subject of lively debate, even for the two "simpler" and more thoroughly studied nucleobases, namely, uracil (U) and thymine (5-methyluracil).[30,40]

In fact, different computational methods agree in predicting that two excited states, a dark one with $n\pi^*$ character (hereafter Sn) and a bright one with $\pi\pi^*$ character ($S\pi$), lie close in energy in the FC region.[29,45] Concerning the gas phase, there is strong disagreement on the relevance of the Sn/$S\pi$ crossing in the excited-state dynamics, on the existence of a minimum on $S\pi$ (and on their eventual geometry and stability with respect to Sn), on the role played by the $S\pi$ minimum in the dynamics, and on the possible participation of an additional bright state (involving the carbonyl double bond) in the excited-state decay.[32,35−38,45] The mechanism of the excited-state dynamics in solution is less debated, probably due to the smaller number of theoretical studies of pyrimidine excited states including solvent effects.[13,14,34,43−46] Experiments and computations agree in predicting a very fast $S\pi \rightarrow S_0$ decay, on the subpicosecond time scale, for uracil and thymine although a significant part of the excited-state population is trapped within the Sn dark state.[11−14,34,46]

In such a scenario, investigating the excited-state behavior of uracil derivatives is particularly useful. Indeed, assessing the substituent effect on the excited-state behavior can provide interesting insights into the microscopic radiative and nonradiative mechanisms and into the underlying chemical physical effects. Furthermore, it provides a fundamental check of the accuracy of the different quantum mechanical methods used for treating the excited-state behavior of the nucleobases. In this respect, our preliminary study of 5-aminouracil (5 AU) and

* Corresponding author. E-mail: robimp@unina.it; roberto.improta@cea.fr.
[†] CEA/DSM/IRAMIS/SPAM - CNRS URA 2453.
[‡] Present address: Matiere Molle et Chimie (ESPCI-CNRS, UMR 7167), ESPCI, 75231 Paris Cedex 05, France.
[§] Universitat Rovira i Virgili.
[||] Istituto Biostrutture e Bioimmagini-CNR.

10.1021/jp105267q
Published on Web 09/10/2010

SCHEME 1: Schematic Structures of the Two Aminosubstituted Uracils Studied[a]

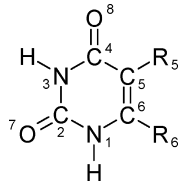

[a] 5 AU: $R_5 = NH_2$, $R_6 = H$; 6 AU: $R_5 = H$, $R_6 = NH_2$.

6-aminouracil (6 AU), Scheme 1, indicates that these two compounds can be very effective "test cases" for studying substituent effect.[58] Their excited-state decay is indeed completely different from other uracils, providing a very impressive demonstration of the huge effect that the nature and the position of the substituents have on the photophysical properties of uracils. The fluorescence of 6 AU decays as fast as that of uracil with a time constant of about 100 fs or less. The fluorescence of 5 AU exhibits instead a much more complex behavior, fundamentally different from what we found in any other uracils: the decays are globally slower (up to several picoseconds) and depend strongly on the wavelength.

We here report a thorough theoretical and experimental study of the steady-state absorption and fluorescence spectra of 5 AU and 6 AU in water, and we compare them with those of U. To discriminate between intrinsic and environmental effects, our computational study has been performed both in the gas phase and in aqueous solution, by using both CASPT2/CASSCF and TD-DFT calculations. Calculations in water have been performed at the TD-DFT level, including the bulk solvent effect by using the polarizable continuum model (PCM),[59,60] both in its linear response (LR-PCM)[61] and in its state-specific (SS-PCM) implementations.[62,63] The effect of explicit solute−solvent interactions has been taken into account by including several water molecules of the first solvation shell (from 1 to 8; see below) in the calculations.

We here show that the steady-state absorption and fluorescence spectra of 5 AU and 6 AU exhibit fundamental differences with respect to those of U (Figure 1). Our computational results are in good agreement with experiments, and provide interesting indications on the effects modulating the excited-state behavior of uracil derivatives as well as additional hints on the mechanism of their decay. Furthermore, useful information on the performances of the different quantum mechanical methods in treating the substituent effect on the pyrimidine excited electronic states has been obtained.

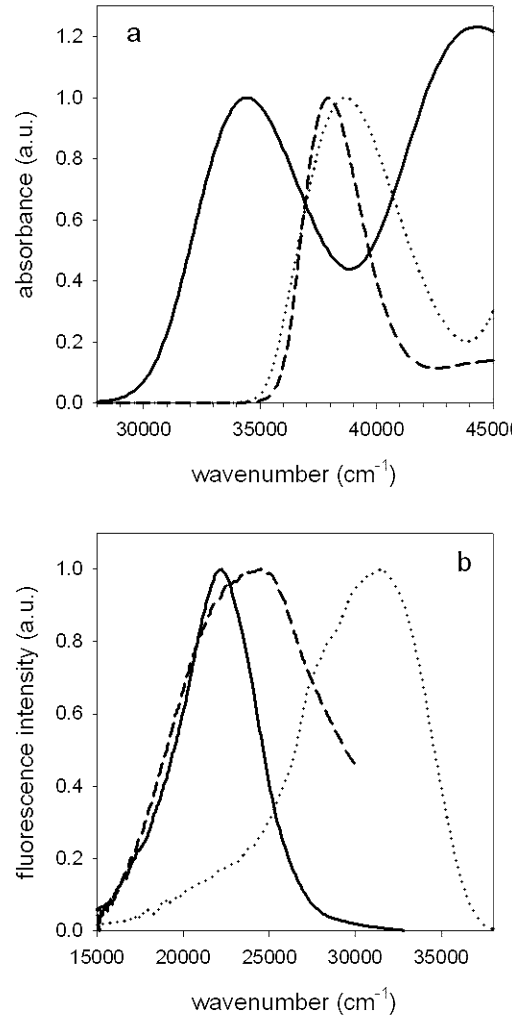

Figure 1. Experimental normalized absorption (a) and fluorescence (b) spectra of U (dotted), 5 AU (solid), and 6 AU (dashed) in aqueous solution.

2. Computational and Experimental Details

2.1. Computational Details. ***PCM/TD-DFT Calculations.*** The PBE0[64−66] exchange−correlation functional has been used for ground- (PCM/PBE0 calculations) and excited-state (PCM/TD-PBE0 calculations) geometry optimizations. The absorption and emission transitions were calculated by the TD-DFT[67,68] method using the PBE0 and CAM-B3LYP[69,70] functionals. Both 6-31G(d) and 6-31+G(d,p) basis sets have been employed in the geometry optimizations on 5 AU and 6 AU, providing similar results (see Supporting Information). As a consequence, the geometry optimizations of the models including the water molecules of the cybotactic region have been performed at the less computationally demanding 6-31G(d) level. In any case, the vertical absorption ν_A and emission energies ν_E have always been refined by single-point calculations employing more extended 6-31+G(d,p) and 6-311+G(2d,2p) basis sets.

This approach has already been successfully applied for nucleobase excited states and it has been shown to provide very accurate vibrationally resolved spectra for several classes of compounds.[71−75] All the computed vibrational frequencies in the minima of the ground and excited states (computations made for the systems containing up to 1 water molecule) are positive, the only exception concerns 5 AU·7(H_2O) and 6 AU·8(H_2O), where librational modes of water can exhibit small (<50 cm^{-1}) imaginary frequencies. In each case we checked that our conclusions are not affected by small variations in the geometry of the solvation shell.

Bulk solvent effects on the electronic states are accounted for with the polarizable continuum model (PCM).[59,60] The excitation and emission energies, ν_A and ν_E, are computed with the "standard" linear response (LR) implementation of PCM/TD-DFT (which has been also used in the excited-state geometry optimizations)[61] and the new state-specific (SS) one, which allows for better treatment of the dark and bright transitions and is mandatory for a rigorous treatment of dynamical solvation effects.[62,63]

Our previous work indicates that an accurate satisfactory treatment of the pyrimidine excited states in aqueous solution requires inclusion of water molecules in the first solvation shell.[13,14,34,43] Here the PCM calculations have thus been performed including a number of H_2O molecules varying (see

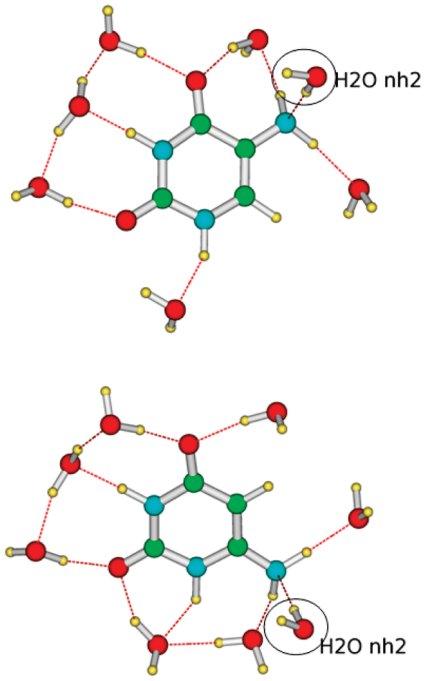

Figure 2. Computational models used for studying 5 AU (up) and 6 AU (bottom) in aqueous solution. In 5 AU·1(H_2O) and 6 AU·1(H_2O) only the H_2O_{nh2} is included. In 5 AU·6(H_2O) and 6 AU·7(H_2O) all the water molecules but H_2O_{nh2} are included. In 5 AU·7(H_2O) and 6 AU·8(H_2O) all the water molecules are included.

Figure 2) between 0 and 7 (for 5 AU) and 8 (for 6 AU). In the excited-state geometry optimizations the first solvation shell was fully optimized, i.e., was treated like solute degrees of freedom. Since outer solvation shells are not included in our calculations, the conformational flexibility of the water molecules of the cybotactic region could be overestimated. As a consequence, the computed emission energies represent a lower bound of the experimental ones.

The simplest way of taking into account dynamical solvation effects on absorption and emission energies is to use two limiting cases, the nonequilibrium (NEQ) and equilibrium (EQ) time regime. In the NEQ case, only fast solvent degrees of freedom (corresponding to electronic polarization) are in equilibrium with the molecular excited-state density, whereas, in the EQ regime, also nuclear polarizations (slow solvent degrees of freedom) are equilibrated. For calculating absorption energies ν_A the NEQ limit is more suitable, while for emission ν_E the EQ regime must be used.[59,60] While such an approach is obviously valid for long-lived excited states it may be questionable for the very short-lived excited states of U and 6 AU. We believe that the main part of the solvent relaxation is much faster than the excited-state lifetimes of U and 6 AU. The solvation dynamics of water is known to be dominated by a 20 fs component,[76] which is well below the timescales involved for the fluorescence discussed here. In any case in Table 8 we report also the values of the emission energy computed in the NEQ limit.

All the PCM/DFT and PCM/TDDFT calculations have been performed by using a development version of the Gaussian program.[77]

CASSCF/CASPT2 Calculations. All geometries have been optimized using the complete active space self-consistent field method (CASSCF). The nature of the stationary points located has been checked with their harmonic vibrational frequencies. Conical Intersections have been located at the CASSCF level using the method of Bearpark at al.[78]

The energies of the stationary points were recalculated at the complete active space perturbation theory to second-order (CASPT2) level, based on the CASSCF wave function, in the single-state (SS) and multistate (MS) approaches (as implemented in Molcas package), to integrate the effects of the dynamic correlation of the valence's electrons. All geometry optimizations at the CASSCF level have been performed with valence double-ζ basis set 6-31G(d), while for the computation of the energies at the CASPT2 level a ANO basis set has been used.

All CASPT2 calculations have been done with the standard zeroth-order Hamiltonian used in MOLCAS 7.0, that is the ionization potential-electronic afinity (IPEA) modified H_0 with a shift parameter of 0.25 by default. In every case, an imaginary level-shift correction of 0.2 was included in the CASPT2 single point calculations to avoid the presence of intruder states. This value was chosen in agreement with previous calculations performed by our group in the study of uracil,[46] where this value proved to be appropriate. The oscillator strengths were calculated with Molcas with the CASCI method using the perturbed modified CASSCF (PM-CASSCF) wave function given by the CASPT2 module.

In CASSCF as well as in CASPT2 calculations, different active spaces were used. The largest one, a (16,11) active space, was used for optimizations of the ground-state and of the two first excited-state minima at the CASSCF level. This CAS includes all valence orbitals: eight π electrons and the lone pairs of the amino substituent and of the two n_O orbitals. Given that the $n_{O7}-\pi^*$ excitation is higher in energy than the excited states of interest (like in the case of uracil), as shown in the CASSCF results, the n_{O7} orbital has been taken out of the active space for the CASPT2 single point calculations, where a (14,10) active space was then used. It reduces the cost of the CASPT2 calculations, allows us to compare these results with the ones of our previous work on uracil, and avoids problems of orbitals switch during the orbital optimization step.

It is worthy to note, from the results presented in the next section, that in general, for the three molecules here considered, the dynamic electronic correlation has a quite large effect on the energetics of the Sπ states, while for the Sn state the effect is almost negligible. This aspect makes the value computed at the CASPT2 level much more reliable for the Sn state than for the other two states.

Geometry optimizations at the CASSCF level were conducted with the Gaussian 03 package, while CASPT2 single point calculations were done with the MOLCAS 7.0 package.[79] For the ground-state structure of the 5 AU, two minima were found, one with the amino group almost coplanar with the ring, and another with the substituent rotated in an almost perpendicular orientation (see the Supporting Information). Although the first geometry is in agreement with the experimental results, it is an unstable structure, as it corresponds to a shallow minimum 1.4 kcal mol^{-1} less stable (at the CASSCF/6-31G* level) than the rotated minimum. The inclusion of an explicit water molecule in the description of the system was shown to avoid this problem, making the planar minimum more stable, so all the calculations have been done in this way. To keep the comparability, this water molecule was also included in the 6 AU system. To check the possible influence of this water molecule in the results, several test calculations were performed of the "nude" uracil derivatives. First of all, some geometries of stationary points of the 6 AU PES were reoptimized without the explicit water molecule, finding negligible changes in the geometrical parameters. Then the relative energies of different

states at fixed geometries and relative energies of different areas of the PES were compared for both 6 AU and 5 AU, with and without the explicit water molecule, and again no significant differences were found. Consequently, given that the results show that the inclusion of one water molecule does not change significantly the relative energies for both system or the geometries in the case of 6 AU, all the energetic data reported in this paper at the CASPT2/CASSCF level are referred to the 5 AU·H_2O and 6 AU·H_2O systems. It has to be pointed out that the position of this water molecule is quite different from those included in the PCM/DFT study (see the Supporting Information).

2.2. Material and Experimental Methods. 5-Aminouracil (5 AU) and 6-aminouracil (6 AU), Scheme 1, were purchased from Sigma Aldrich and used without further purification. They were dissolved in ultrapure water produced by a MILLIPORE (Milli-Q Synthesis) purification system. For the absorption spectra about 8×10^{-4} M solutions were used both for 5 AU and for 6 AU. For the fluorescence spectra a 2×10^{-4} M solution was used for 5 AU while for 6 AU the concentration was 2×10^{-5} M.

Absorption spectra were recorded with a Perkin Lambda 900 spectrophotometer using 1 mm quartz cells (QZS). The oscillator strength was calculated by

$$f_{mn} = \left[\frac{4\varepsilon_0 m_e c^2 \ln(10)}{N_A e^2}\right] A \qquad (1)$$

where the bracket has the value of 4.319×10^{-9} mol dm^{-3} cm^2 and A is the band integral.

Fluorescence spectra were recorded with a SPEX Fluorolog-3 spectrofluorometer, equipped with a 450 W arc Xenon lamp, using 10 mm quartz cells (QZS). The excitation wavelength used was 255 nm. To obtain an acceptable signal-to-noise ratio, several tens of recordings were averaged and the baseline from neat water was subtracted. The fluorescence spectra were corrected for the spectral sensitivity of the apparatus.

The fluorescence quantum yields were calculated by

$$\phi_X = \frac{A_X}{A_S}\frac{(1 - 10^{-OD_S})}{(1 - 10^{-OD_X})}\phi_S \qquad (2)$$

where A is the area of the spectrum and OD is the optical density of the solution at the exciting wavelength. The subscripts X and S denote respectively the compound under study and TMP, which was used as secondary standard. The fluorescence quantum yield of TMP/H_2O with $\lambda_{exc} = 255$ nm is 1.54×10^{-4}.[80]

3. Results

3.1. Experimental Absorption and Fluorescence Spectra. The steady-state absorption spectra of 5 AU, 6 AU, and U in aqueous solution are reported in Figure 1, and the most significant experimental characteristics are summarized in Table 1. It is clear that the absorption spectrum of 5 AU is extremely different with respect to that of U. For the lowest energy absorption band it can be observed that (i) the maximum is significantly red-shifted, by about 0.5 eV ($\sim 4 \times 10^3$ cm^{-1}), (ii) it is much broader (5.8×10^3 vs 4.9×10^3 cm^{-1}), and (iii) the peak extinction coefficient is much lower (5.9×10^3 at 290 nm for 5 AU vs 9.1×10^3 M^{-1} cm^{-1} at 259 nm for U). Moreover, a higher transition, being more intense than the lowest energy one, can be observed at ca. 5.6 eV.

TABLE 1: Characteristic Parameters of the First Absorption and Fluorescence Bands of Uracil and Its Amino Derivatives[a]

	absorption			fluorescence			
	ε_{max}	λ_{max}	ν_{max}	$10^4\Phi_F$	λ_{max}	ν_{max}	$\Delta\nu$
U[b]	*9.1*	*259*	*38.6 (4.8)*	*0.35*	*312*	*31.3 (3.9)*	*7.3 (0.9)*
5 AU	5.9	290	34.5 (4.3)	6	446	22.2 (2.8)	12.3 (1.5)
6 AU	24.6	264	38.0 (4.7)	0.5	397	24.5 (3.0)	13.5 (1.7)

[a] The peak molar extinction coefficient ε_{max} (10^3 M^{-1} cm^{-1}), the peak wavelength λ_{max} (nm), the peak frequency ν_{max} (10^3 cm^{-1} (eV in parentheses)), the fluorescence quantum yield Φ_F, and the Stokes shift $\Delta\nu$ (peak absorption minus peak fluorescence) (10^3 cm^{-1} (eV in parentheses)). Literature data are shown in italics. [b] From ref 13.

The lowest energy absorption spectrum of 6 AU is instead more similar to that of U, its maximum being red-shifted by only 0.08 eV. On the other hand, it is much sharper (3×10^3 cm^{-1}) than that of U and the peak extinction coefficient is more than twice as large (24.6×10^3 M^{-1} cm^{-1} at 264 nm) as that of U. A higher transition is also present at ca. 220 nm, but it is significantly less intense than the lowest energy one.

The first absorption bands of 5 AU and 6 AU were lognorm-fitted, allowing a straightforward integration on a wavenumber scale. The band integrals were 3.68×10^7 dm^3 mol^{-1} cm^{-2} for 5 AU and 7.97×10^7 dm^3 mol^{-1} cm^{-2} for 6 AU (see Figure S2, Supporting Information). From these values the corresponding oscillator strengths were calculated using eq. 1: they are 0.16 for 5 AU and 0.34 for 6 AU.

Taking uracil as a reference, 5 AU and 6 AU exhibit opposite behaviors. These results confirm that the excited-state behavior of uracil derivatives is sensitive not only to the nature of the ring substituents but also to their positions, even for C_5 and C_6 that are engaged in the same double bond. Regarding the nature of the substituents, on the other hand, an amino group in the 6-position leads to more significant changes than a methyl substituent in the same position. The absorption spectrum of 6-methyluracil is in fact extremely similar to that of U.

Inspection of the steady-state fluorescence spectra (see Figure 1 and Table 1) confirms these considerations. In fact, the emission maximum of 6 AU and in particular that of 5 AU are remarkably red-shifted with respect to that of U. Consequently, the Stokes shifts for both 5 AU and 6 AU are extremely large, ca. 12.3×10^3 and 13.7×10^3 cm^{-1}, respectively, i.e., almost twice as large as that of U (7.3×10^3 cm^{-1}). Interestingly, the fluorescence spectrum of 5 AU is significantly sharper, and that of 6 AU much broader than that of U. It should be noted that the 6 AU emission spectrum also exhibits a distinct shoulder around 32×10^3 cm^{-1}, close to the emission maximum of uracil. The fluorescence quantum yields for 5 AU and 6 AU were calculated to be 6×10^{-4} and 5×10^{-5}, respectively.

3.2. Computed Absorption Spectra in the Gas Phase. As a first step of our computational study of 5 AU and 6 AU, we have computed their lowest vertical excitation energies in the gas phase, both at the TD-DFT (PBE0 and CAM-B3LYP functionals) and at the MS-CASPT2 levels (see Tables 2 and 3). Calculations indicate that the two lowest energy excited states of 6 AU and 5 AU are qualitatively similar to that of U.[13,14,33,45] Indeed, a bright transition with $\pi\pi^*$ character is predicted, which can be described as a HOMO−LUMO excitation (the frontier orbitals obtained at the PBE0/6-31G(d) level are schematically depicted in Figure 3). The HOMO and the LUMO can be related to bonding/antibonding π and π^* orbitals of the C_5C_6 ethylenic

TABLE 2: Vertical Excitation Energies ν_A (eV) of 5 AU, 6 AU, and U Computed in the Gas Phase at the TD-PBE0 and the TD-CAM-B3LYP Levels, Using the Geometries Optimized at the PBE0/6-31+G(d,p) Level (Oscillator Strengths in Parentheses)

	5 AU			6 AU			U		
	6-31G (d)	6-31+G (d,p)	6-311+G (2d,2p)	6-31G (d)	6-31+G (d,p)	6-311+G (2d,2p)	6-31G (d)	6-31+G (d,p)	6-311+G (2d,2p)
					PBE0				
Sπ	4.48 (0.12)	4.30 (0.13)	4.24 (0.12)	5.58 (0.21)	5.45 (0.21)	5.40 (0.18)	5.44 (0.13)	5.33 (0.15)	5.25 (0.14)
Sn	5.13 (0.00)	5.09 (0.00)	5.06 (0.00)	5.13 (0.00)	5.14 (0.00)	5.11 (0.00)	4.79 (0.00)	4.80 (0.00)	4.77 (0.00)
Sπ1	5.91 (0.20)	5.71 (0.15)	5.66 (0.18)	6.39 (0.07)	6.12 (0.06)	6.07 (0.06)	6.20 (0.04)	6.12 (0.04)	6.06 (0.04)
					CAM-B3LYP				
Sπ	4.68 (0.15)	4.47 (0.16)	4.40 (0.15)	5.69 (0.25)	5.54 (0.21)	*b*	5.61 (0.17)	5.47 (0.20)	5.38 (0.18)
Sn	5.31 (0.00)	5.29 (0.00)	5.27 (0.00)	5.36 (0.00)	5.37 (0.03)	5.35 (0.04)	5.05 (0.00)	5.07 (0.00)	5.05 (0.00)
Sπ1	6.22 (0.21)	6.02 (0.22)	*a*	6.84 (0.11)	6.51 (0.10)	6.38 (0.05)	6.68 (0.04)	6.59 (0.04)	6.52 (0.04)

[a] Two transitions at 5.92(0.09) and at 5.96 (0.12). [b] Coupled with a Rydberg states: two transitions at 5.41(0.12) and 5.52 (0.11).

TABLE 3: Vertical Excitation Energies (eV) Computed at the CASPT2(14,10)/ANO Level on CASSCF(16,11)/6-31G(d) Optimized Geometries (State Averaged Results for Four Roots of Equivalent Weight)

	CASSCF	CASPT2	MS-CASPT2	f^a
		5 AU		
Sπ	6.29	4.40	4.42	0.256
Sn	5.47	5.45	5.50	0.000
Sπ1	7.57	6.38	6.58	0.109
		6 AU		
Sπ	6.66	5.23	5.42	0.544
Sn	5.45	5.51	5.61	0.000
Sπ1	7.73	6.80	6.93	0.040
		U[b]		
Sπ	6.56	5.14	5.22	0.323
Sn	5.00	5.00	5.08	0.000
Sπ1	7.09	6.19	6.28	0.030

[a] Oscillator strength from CASCI calculations. [b] CAS (12/9).

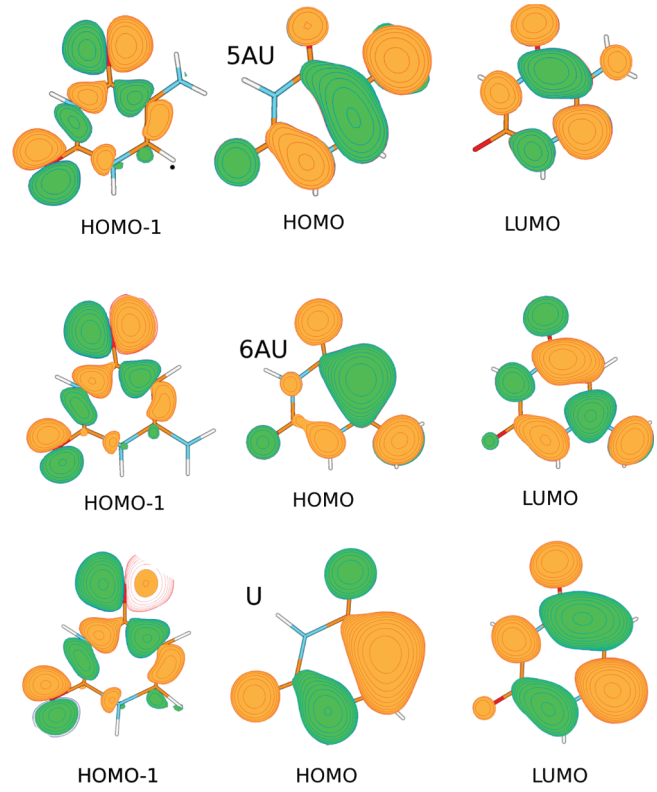

Figure 3. Frontier orbitals of AU, 6 AU, and 5 U obtained at the PBE0/6-31G(d) level. Green/orange colors are relative to the sign of the atomic orbitals within each MO, enabling us to judge the bonding/antibonding character of each MO with respect to each bond.

moiety. Close in energy to this bright transition, calculations predict the existence of a dark transition with nπ* character, corresponding to the excitation from the HOMO−1 (the combination of the lone pairs, LP, of the two carbonyl moieties) to the π* LUMO. In analogy with the nomenclature used in our previous studies of uracil derivatives, we label the excited states related to these transitions as Sπ and Sn, respectively.[13,14,44−46] Inspection of Figure 3 shows that the frontier orbitals of 5 AU and 6 AU are qualitatively similar to that of U, but both the HOMO and the LUMO contain significant contributions of the LP of the amino substituent.

As a matter of fact, calculations, in agreement with the experimental results, indicate that the amino substituent significantly affects the properties of the lowest energy excited states of U. For 5 AU both TD-DFT (independently of the functional and of the basis set adopted) and CASPT2 calculations predict that the lowest energy excited state is Sπ, whose transition energy is significantly red-shifted (by ∼1 eV) with respect to the corresponding transition in U. Inspection of the frontier orbitals in Figure 3 shows indeed that in 5 AU the contribution of the LP of the amino substituent to the HOMO and the LUMO is antibonding with respect to that of the C_5 atom, and as a consequence, we can expect that these orbitals are destabilized with respect to their counterparts in U. On the other hand, the contribution of the LP and, consequently, its destabilizing effect is much larger for the HOMO, leading to the decrease of the HOMO−LUMO gap and to the significant red shift of the transition energy. The presence of another bright transition ($S_0 \rightarrow S\pi1$), more intense and blue-shifted by ∼1.5 eV with respect to $S_0 \rightarrow S\pi$, is also correctly predicted by TD-DFT and MS-CASPT2 calculations, although this latter method does not correctly reproduce the relative intensities of these bands.

5-Amino substitution alters also the energy ordering of the Sπ and Sn excited states. While in U the latter is significantly more stable than the former, at least in the gas phase, for 5 AU Sπ is predicted to be the lowest energy excited state in vacuo.

From the quantitative point of view, it is noteworthy that computations significantly overestimate the effect of the 5-amino substituent on the absorption spectra, since the predicted red shift of the $S_0 \rightarrow S\pi$ transition energy is twice as large as that found experimentally in water (both according to the gas phase TD-PBE0 and MS-CASPT2 calculations).

Calculations confirm instead that an amino substituent in position 6 does not have a dramatic effect on the uracil absorption spectrum so the energy of the $S_0 \rightarrow S\pi$ transition in 6 AU is rather similar to that found in U. As shown in Figure 3, for 6 AU the antibonding contribution of the amino substituent

TABLE 4: Vertical Excitation Energies (eV) of 5 AU, 6 AU, and U Computed in Water at the PCM-TD-PBE0 Level, Using the Geometries Optimized at the PCM/PBE0/6-31+G(d,p) Level (Oscillator Strengths in Parentheses)[a]

	5 AU			6 AU			U		
	6-31G (d)	6-31+G (d,p)	6-311+G (2d,2p)	6-31G (d)	6-31+G (d,p)	6-311+G (2d,2p)	6-31G (d)	6-31+G (d,p)	6-311+G (2d,2p)
Sπ	4.36 (0.15)	4.20 (0.17)	4.14 (0.15)	5.47 (0.29)	5.28 (0.35)	5.24 (0.34)	5.33 (0.18)	5.21 (0.21)	5.14 (0.20)
Sn	5.22 (0.00)	5.27 (0.00)	5.24 (0.00)	5.54 (0.00)	5.64 (0.00)	5.62 (0.00)	5.04 (0.00)	5.13 (0.00)	5.11 (0.00)
Sπ1	5.72 (0.28)	5.51[b] (0.30)	5.46[b] (0.28)	6.07 (0.08)	5.76 (0.10)	5.72 (0.10)	6.34 (0.07)	6.29 (0.13)	6.24 (0.11)

[a] Experimental absorption maxima: 5 AU = 4.26 eV, 6 AU = 4.70 eV, U = 4.79 eV. [b] S4, S2 is a Rydberg state.

TABLE 5: Vertical Excitation Energies (eV) of 5 AU and 6 AU Computed in Water Solution at the PCM/TD-PBE0 Level, Including Some Water Molecules of the First Solvation Shell, Using the Geometries Optimized at the PCM/PBE0/6-31G(d) Level (Oscillator Strengths in Parentheses)

	6-31G (d)	6-31+G (d,p)	6-311+G (2d,2p)	6-31G (d)	6-31+G (d,p)	6-311+G (2d,2p)
		5 AU·1(H_2O)			6 AU·1(H_2O)	
Sπ	4.57 (0.17)	4.41 (0.18)	4.34 (0.17)	5.39 (0.16)[a]	5.26 (0.33)	5.22 (0.32)
Sn	5.26 (0.00)	5.29 (0.00)	5.26 (0.00)	5.43 (0.13)[a]	5.52 (0.00)	5.50 (0.00)
Sπ1	5.90 (0.28)	5.69 (0.29)	5.64 (0.27)	6.28 (0.11)	5.98 (0.13)	5.93 (0.12)
		5 AU·6 (H_2O)			6 AU·7(H_2O)	
Sπ	4.09 (0.13)	3.98 (0.15)	3.94 (0.14)	5.40 (0.34)	5.24 (0.39)	5.20 (0.38)
Sn	5.49 (0.00)	5.49 (0.00)	5.45 (0.00)	5.96 (0.00)	5.96 (0.00)	5.94 (0.00)
Sπ1	5.43 (0.31)	5.27 (0.30)	5.22 (0.29)	5.80 (0.07)	5.57 (0.07)	5.52 (0.07)
		5 AU·7 (H_2O)			6 AU·8(H_2O)	
Sπ	4.30 (0.15)	4.19 (0.16)	4.14 (0.15)	5.33 (0.35)	5.21 (0.38)	5.17 (0.37)
Sn	5.46 (0.00)	5.46 (0.09)[a]	5.43 (0.00)	5.81 (0.00)	5.83 (0.00)	5.82 (0.00)
Sπ1	5.60 (0.31)	5.46 (0.19)[a]	5.41 (0.26)	5.95 (0.08)	5.71 (0.09)	5.67 (0.09)
		U·4 (H_2O)				
Sπ	5.27 (0.19)	5.17 (0.22)	5.10 (0.20)			
Sn	5.31 (0.00)	5.34 (0.00)	5.32 (0.00)			

[a] Strong mixing.

to the HOMO is similar to that of the LUMO, leading to a much smaller variation of the HOMO−LUMO gap than was found for 5 AU. On the other hand, a quantitative disagreement is found for 6 AU: the $S_0 \rightarrow S\pi$ transition is predicted to be slightly blue-shifted (by 0.1 eV according to TD-PBE0 and by 0.2 eV according to MS-CASPT2) with respect to U, while the experimental band maximum is red-shifted by 0.1 eV.

Regarding the Sn state, TD-DFT and MS-CASPT2 results predict that this state is the lowest energy excited state of 6 AU, like in U.[13,14,33,45] The contribution of the amino substituent to the HOMO−1 is very small, and thus the $S_0 \rightarrow$ Sn transition is blue-shifted relative to uracil due to the destabilization of the LUMO.

Calculations fully agree with the experiments, instead, concerning the substituent effect on the intensity of the lowest energy bright transitions. Steady-state absorption spectra indicate that the extinction coefficient of the 6 AU band is remarkably larger than that of U, whereas that of the 5 AU band is smaller. This trend is fully reproduced by the TD-DFT and MS-CASPT2 results already in the gas phase, although the experimentally observed substituent influence on the intensities is much more important.

3.3. Computed Absorption Spectra in Aqueous Solution. The picture obtained in the gas phase is not qualitatively changed by the inclusion of bulk solvent effects by the PCM model (see Tables 4 and S2−S3 in the Supporting Information). Confirming the results obtained on other uracil derivatives,[13,14,43−45] Sn is destabilized in aqueous solution with respect to Sπ. For 5 AU, a strong peak is predicted at the TD-PBE0 level at ∼4.2 eV (corresponding to the $S_0 \rightarrow S\pi$ transition) and another, more intense, absorption band at ∼5.5 eV ($S_0 \rightarrow S\pi1$ transition). For 6 AU, TD-PBE0 calculations predict a very intense absorption band at 5.2 eV and a weaker one in its blue tail. TD-CAM-B3LYP calculations (see Supporting Information) provide indications similar to those of TD-PBE0. As already discussed in the previous section, the general description of the 5 AU and 6 AU absorption spectra is in good agreement with experiments, except for the overestimation of the red shift of the $S_0 \rightarrow S\pi$ transition in 5 AU and especially in 6 AU, with respect to U.

Confirming our previous computational results,[13,14,43−46] the inclusion of the water molecules of the first solvation shell has a limited effect on the energy of the Sπ excited state, which exhibit a weak red shift, while it leads to a significant destabilization of the Sn excited state (see Tables 5 and 6), given that the transfer of an electron from the carbonyl LP to the more diffuse π^* orbital causes the weakening of the hydrogen bonds with the water molecules.[13,14,43−46] On the other hand, it is important to highlight that the presence of a water molecule perpendicular to the molecular plane, acting as hydrogen bond donor with respect to the nitrogen lone pair of the amino substituent, significantly modulates the absorption spectra of 6 AU and, especially, of 5 AU. In this latter compound the inclusion of this water molecule in the calculations leads to a blue shift of the Sπ ν_A of 0.2 eV at the PCM/TD-PBE0/6-31+G(2d,2p) level of calculation (see Tables 4 and 5), in much better agreement with the experiments. For 5 AU·1(H_2O), the computed ν_A is 4.34 eV, red-shifted by 0.8 eV with respect to the Sπ ν_A in U, reducing the discrepancy with respect to the corresponding experimental absorption peaks to less than 0.3 eV. The interaction with the surrounding water molecules can thus decrease the interaction between the nitrogen LP and the pyrimidine ring, and, thus, its influence on the ν_A. We underline that the oscillator strengths calculated in solution compare very well with the experimentally determined ones: 0.16 for 5 AU and 0.34 for 6 AU, regardless of the method used.

TABLE 6: Vertical Excitation Energies (eV) of 5 AU and 6 AU Computed in Water Solution at the PCM/TD-CAM-B3LYP Level, Including Some Water Molecules of the First Solvation Shell, Using the Geometries Optimized at the PCM/PBE0/6-31G(d) Level (Oscillator Strengths in Parentheses)

	6-31G (d)	6-31+G (d,p)	6-311+G (2d,2p)	6-31G (d)	6-31+G (d,p)	6-311+G (2d,2p)
		5 AU ·1(H_2O)			6 AU ·1(H_2O)	
Sπ	4.76 (0.20)	4.51 (0.21)	4.49 (0.20)	5.48 (0.33)	5.32 (0.38)	5.27 (0.36)
Sn	5.45 (0.00)	5.52 (0.00)	5.51 (0.00)	5.65 (0.00)	5.76 (0.00)	5.74 (0.00)
Sπ1	6.20 (0.29)	5.96 (0.30)	5.89 (0.29)	6.68 (0.15)	6.26 (0.16)	6.20 (0.15)
		5 AU·6 (H_2O)			6 AU ·7(H_2O)	
Sπ	4.26 (0.17)	4.14 (0.18)	4.08 (0.17)	5.44 (0.39)	5.26 (0.44)	5.23 (0.43)
Sn	5.72 (0.00)	5.73 (0.00)	5.70 (0.00)	6.21 (0.03)	5.92 (0.01)	5.90 (0.001)
Sπ1	5.69 (0.33)	5.52 (0.32)	5.47 (0.29)	6.23 (0.08)	5.90 (0.09)	5.84 (0.09)

TABLE 7: CASPT2 and TDPBE0 Absorption ν_A and Emission ν_E Energies (eV) and Stokes Shift $\Delta\nu$ (Peak Absorption Minus Peak Fluorescence) (10^3 cm^{-1}) (Oscillator Strengths in Parentheses)

	5 AU			6 AU		
	ν_A	ν_E	$\Delta\nu$	ν_A	ν_E	$\Delta\nu$
			Gas Phase			
CASSCF	6.29	5.00	10400	6.66	directly to CI	
CASPT2	4.40	3.29	8950	5.23		
MSCASPT2	4.42 (0.26)	3.33 (0.28)	8800	5.42 (0.54)		
TD-PBE0	4.30 (0.13)	3.27 (0.10)	8300	5.45 (0.21)	directly to CI	
			Water - TD-PBE0[a]			
water PCM	4.20 (0.17)	3.29 (0.14)	7300	5.28 (0.35)	3.55[b] (0.16)	13950
water PCM + 1 H_2O	4.39 (0.18)	3.36 (0.14)	8300	5.24 (0.33)	3.66[b] (0.16)	12750
water PCM + 6/7 H_2O	3.98 (0.14)	3.08 (0.12)	7250	5.24 (0.39)	directly to CI	

[a] TD-PBE0 Results Computed in Water at the LR-PCM/TD-PBE0/631+G(d,p) Level, Using the Geometries Optimized at the PCM/PBE0/6-31+G(d,p) Level. [b] Pseudominimum, 1/2 low-energy negative frequencies.

3.4. Computed Emission Spectra. To interpret the experimental fluorescence spectra, it is important to focus on the lowest energy bright state. This state, Sπ, is expected to play a dominant role in fluorescence for two reasons: (1) it corresponds to an allowed ("bright") transition and (2) calculations predict the "dark" Sn state to be located well above the Sπ state for both 5 AU and 6 AU in aqueous solution. We thus limit our analysis to the study of the Sπ minima. Before analyzing the behavior of the two aminouracils, it is useful to briefly recall the picture obtained earlier for U. For this compound PCM/TD-PBE0/6-31G(d) geometry optimizations in aqueous solution predict the existence of a very shallow minimum, in which the pyrimidine ring assumes a "boat-like" conformation.[13,14,34,45,46] In this minimum N_3 and C_6 are out of the plane defined by N_1, C_2, C_4, and C_5, whereas the oxygen and hydrogen atoms exhibit small deviation from the planarity. However, experimental Raman resonance (RR)[19−21] experiments combined with an extensive exploration of the Sπ PES[46] show that uracil-like molecules keep the planar geometry they have at the FC point during the first femtoseconds after the excitation to Sπ. Actually, the Sπ minimum of U optimized under the constraint of planarity is only <0.05 eV less stable than the absolute minimum and the bond lengths and the bond angles of these two minima are very similar. As a matter of fact, SS-PCM/TD-PBE0/6-31G(d) and LR-PCM/TD-PBE0/6-31G(d) calculations for U in water predict that the emission from the planar minimum is red-shifted with respect to ν_A by ∼5.5 × 10^3 cm^{-1}, a value rather close to the experimental Stokes shift (7.3 × 10^3 cm^{-1}). In any case, these minima actually disappear when a larger basis set is used, and a barrierless path connects the FC region to the CI with the ground electronic state.

For 5 AU and 6 AU our calculations predict a behavior rather different with respect to that just depicted for U. For 5 AU TD-PBE0/6-31G(d) and 6-31+G(d,p) and CASSCF(16,11)/6-31G(d) excited-state geometry optimizations in the gas phase indicate indeed that a stable minimum (hereafter Sπ-min) exists on the Sπ PES. In this minimum the pyrimidine ring exhibits a bent geometry, similar to that found in U, where the molecule can be considered to be divided into two almost planar moieties, defined by the $N_3C_4C_5C_6$ and $N_3C_2N_1C_6$ atoms, respectively, forming an angle of ∼25° at the TD-DFT level, but only of 4° at the CASSCF level. Confirming the results obtained on the other uracil derivatives, the most relevant changes with respect to the ground-state minimum are exhibited by the C_5C_6 bond length (increase of 0.05 Å in both TD-DFT and CASSCF calculations), and noticeable differences are found also for C_4C_5 (−0.03 Å and −0.02 Å for TD-DFT and CASSCF respectively) and C_4O_8 (+0.02 Å) bond lengths. All these geometry changes are in line with the bonding/antibonding character of those bonds in the HOMO and LUMO. It is noteworthy that for uracil in the Sπ minimum the C_5C_6 bond length is elongated by ∼0.1 Å with respect to the S_0 minimum, suggesting a more significant single bond character than in 5 AU. Interestingly, the geometry of the amino substituent is rather different with respect to the S_0 minimum. The C_5-NH_2 bond distance is shortened by ∼0.03 Å both at the TD-DFT and at the CASSCF levels and the hydrogen atoms are closer to be coplanar with the pyrimidine ring. These changes suggest that the interaction between the amino nitrogen LP and the ring MO is stronger in the Sπ excited state, in line with the smaller NC_5 antibonding character of the LUMO than of the HOMO. Due to the significant geometry changes found in the Sπ minimum, the emission energy is significantly red-shifted with respect to the ν_A, with a Stokes shift of ∼8.3 × 10^3 cm^{-1} at the TD-DFT level, and of ∼8.8 × 10^3 cm^{-1} at the CASPT2 level (see Table 7).

Concerning 6 AU, TD-PBE0 and CASSCF geometry optimizations in the gas phase indicate a large driving force toward a strongly nonplanar geometry. In particular, the NH_2 substituent undergoes a large out-of-plane motion, and a steep PES drives the system toward a CI with the ground electronic state. The

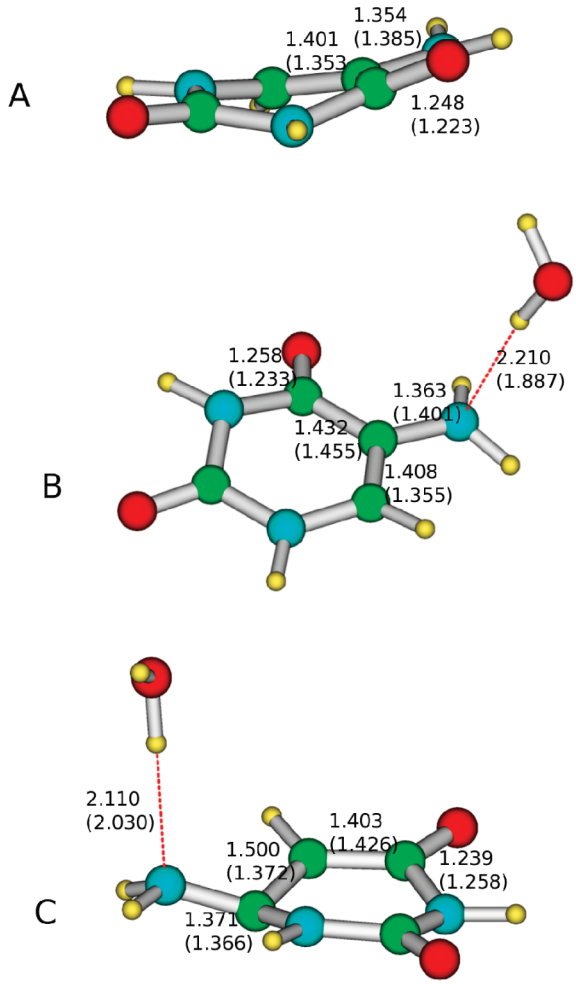

Figure 4. Schematic description and selected degrees of freedom in (a) the Sπ minimum of 5 AU in the gas phase according to TD-PBE0/6-31+G(d,p) geometry optimizations, (b) the Sπ minimum of 5 AU·1(H_2O) in water according to LR-PCM/TD-PBE0/6-31+G(d,p) geometry optimization, and (c) the Sπ pseudominimum of 6 AU·1(H_2O) in water according to LR-PCM/TD-PBE0/6-31+G(d,p) geometry optimization. In parentheses are reported the corresponding values in the S_0 minimum.

CI region is characterized by a strong pyramidalization of the C_5 and C_6 atoms.

PCM calculations in water do not qualitatively change the picture obtained in the gas phase for 5 AU. The presence of a minimum on the Sπ surface is predicted, whose structure is similar to that found in the gas phase. When explicit water molecules are included in the LR-PCM-TDPBE0 calculations, the minimum persists (see Figure 4). The computed Stokes shift is in the range 7.0×10^3 to 8.3×10^3 cm^{-1}. Also in this case, the water molecule hydrogen bonded to the amino nitrogen LP is predicted to be particularly influential, since its presence increases the Stokes shift by 1×10^3 cm^{-1}. Actually, the hydrogen bond between the amino group and the water molecule is significantly weaker in the Sπ-min than in the FC region, as mirrored by the large increase (~0.2 Å) of the hydrogen bond length. This result is in line with the more significant delocalization of the amino LP within the pyrimidine ring in the Sπ excited electronic state.

Solvent effects are instead more influential on 6 AU. In fact, although a fast departure from a planar geometry is predicted for the pyrimidine ring, in line with what was found in the gas phase, PCM/TD-PBE0/6-31+G(d,p) calculations reveal the presence of a quasi-stationary region on Sπ, characterized by a very low gradient (<0.0005 au). In this region the pyrimidine ring exhibits a boat-like structure (see Figure 4c) with a strong pyramidalization of the C_6 and N_3 substituents. A frequency calculation performed for a representative point in this region, i.e., that exhibiting the lowest energy gradient, reveals the presence of one (for 6 AU) and two (for 6 AU 1(H_2O)) low imaginary vibrational frequencies (~-100 cm^{-1}). This point (hereafter Sπ-min*) is not a real Sπ minimum but a saddle point, on the path leading toward the CI, as confirmed by further TD-PBE0 geometry optimizations. In Sπ-min*, the distance between the amino group and hydrogen bonded water molecule is longer than in the ground-state minimum, although the difference is smaller than that found for 5 AU. Due to the significant distortion of the FC geometry, LR-PCM/TD-PBE0 calculations indicate a very large Stokes shift, ca. 13×10^3 cm^{-1}, as shown in Table 7. A much smaller Stokes shift (ca. 5×10^3 cm^{-1}) is instead predicted if the molecule is forced to keep a planar geometry. The experimental fluorescence spectrum of 6 AU, as shown in Figure 1b, is indeed very broad, which may indicate that it contains contributions from a planar region, close to the FC point.

LR-PCM/TD-PBE0 calculations on Sπ-min (for 5 AU) and Sπ-min* (for 6 AU) thus predict large Stokes shifts, in line with the experimental results. However, the LR-PCM method cannot be considered to be the reference choice for computing emission energies, due to its unsuitable treatment of dynamical solvent effect.[62,63,72] As a final step of our analysis, we have thus computed the emission energies for 5 AU and 6 AU by using SS-PCM/TD-PBE0 calculations, which have already been shown to provide a very reliable treatment of fluorescence in solution. As shown in Table 8, independently of the radii adopted in building the PCM cavity, our calculations predict Stokes shifts of 11×10^3 cm^{-1} for 5 AU and of 14×10^3 cm^{-1} for 6 AU, which is in remarkable agreement with the experimental results.

Our computational results can also rationalize the much larger fluorescence quantum yield of 5 AU with respect to 6 AU. In the former compound a true energy minimum exists indeed on the Sπ surface, while in the latter a barrierless path connects the FC region to the CI with S_0.

4. Discussion

Our computational and experimental results confirm that position 5 has a very peculiar role in determining the absorption spectra of uracil derivatives. Inspection of the uracil frontier orbitals shows that the participation of the C_5 and C_6 atomic orbitals to the HOMO is far from being symmetric, the weight of the C_5 AOs being much larger. As a consequence, the energy of the HOMO is much more sensitive to the nature of the C_5 substituent. This feature has already been discussed when the behavior of U was compared with those of thymine (5-methyluracil) and 5-fluorouracil.[13,14,34] It is thus not surprising that the amino substituent, whose LP can take part in the MO of the pyrimidine ring, has such a strong effect on the absorption spectra.

Concerning 5 AU, in its excited state the interaction between the amino group LP and the C_5 carbon atom AO is stronger than in the electronic ground state, since the strong antibonding contribution of the HOMO is partially lost. As a matter of fact, a well-defined minimum is present on the Sπ surface, involving the formation of a partial C_5-N double bond, as witnessed by the significant decrease of the C_5-N bond length and by the planarization of the amino moiety. According to one of the

TABLE 8: Vertical Absorption ν_A and Emission ν_E Energies (in eV, the Energy of S_0 Taken as 0) and Oscillator Strength *f* of the $S_0 \rightarrow S\pi$ Transition for 5 AU and 6 AU in Water[a]

	S_0		nonequilibrium solvation			equilibrium solvation			Stokes shift (cm^{-1})
system	ν_A	*f*	ν_A^{neq}	*f*	ν_E^{neq}	ν_A	*f*	ν_E	$\nu_A - \nu_E$
					5 AU				
UAO	4.24	0.11	3.83	0.10	3.31	3.61	0.09	2.84*	11300
UAHF	4.18	0.11	3.77	0.10	3.20	3.40	0.09	2.81	11000
					6 AU				
UAO	5.64	0.18	5.23	0.12	3.95	5.17	0.11	3.85	14400
UAHF	5.54	0.23	5.05	0.12	4.06	4.93	0.12	3.89	13300

[a] SS-PCM/TD-PBE0/6-31G(d) calculations on geometries computed at the PCM/PBE0/6-31+G(d,p) level.

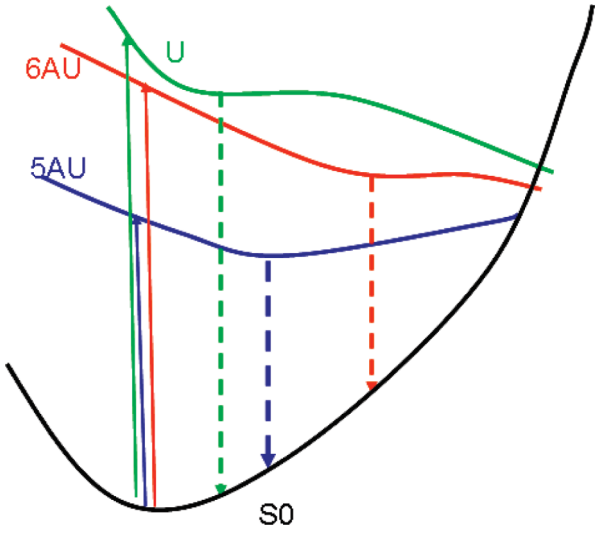

Figure 5. Schematic figure describing the absorption and the emission processes of the bright $S\pi$ state in U (green), 5 AU (blue), and 6 AU (red). Sn states are not described and energy differences are not in scale.

mechanisms proposed for the $S\pi$ excited-state nonradiative decay in uracil derivatives,[13,30,33,35,38] the key motion to reach the CI with the ground state is the pyramidalization of C_5, together with an out-of-plane motion of the C_5 substituent. It is clear that such a process is more difficult for 5 AU than for U, giving account of the much longer excited-state lifetime of the $S\pi$ state in 5 AU, implicitly supporting the likelihood of this mechanism (see Figure 5).

The presence of a minimum on the $S\pi$ surface, whose geometry is noticeably different from that of the ground state, obviously affects the emission energy, explaining the significantly larger Stokes shift of 5 AU and its larger fluorescence quantum yield when compared to those for U.

Regarding 6 AU, TD-DFT and CASPT2 calculations agree in predicting a very fast departure from the ring planarity, with a simultaneous out-of-plane motion of the 6-amino substituent, which finally leads to a CI with S_0. No real energy barrier is predicted for this process (see Figure 5), in line with the ultrafast decay shown by time-resolved experiments. On the other hand, in aqueous solution, PCM-TDPBE0 calculations indicate the existence of a plateau on the $S\pi$ PES, which is likely responsible for the peak observed in the steady-state fluorescence spectrum. This hypothesis is supported by the extremely good agreement found between experimental and calculated (SS-PCM/TD-PBE0) Stokes shifts. Actually, only a multidimensional quantum dynamical study could assess the involvement of this region in the excited-state deactivation path. On the other hand, experiments and computations suggest that a plateau is present also in the lowest energy excited-state PES of guanine in water solution.[28] Also in this case, an out-of-plane motion of the amino substituent is required to reach the CI, suggesting that the rearrangement of the nucleobase's solvation shell could be a relevant factor in modulating deactivation paths involving large scale motion of polar groups.

The involvement of the C_6 substituent in the excited-state decay and the relevance of nonplanar minima with strong pyramidalization at C_6 have already been predicted for the lowest energy states of uracil and thymine (T) in the gas phase, which would adopt a "biradical" electronic structure with a significant involvement of the C_4O_8 double bond, leading to its remarkable lengthening (in a state of $S\pi_O\pi^*$ character).[35,37,50] The nonplanar pseudominimum we found for 6 AU is instead rather similar to the nonplanar minimum evidenced for U and T in solution, exhibiting only a moderate increase of the C_4O_8 bond distance, with no biradical structure and still qualitatively similar to $S\pi$. The most important difference between 6 AU and U concerns the relative weight of the planar and the nonplanar part of the PES in the emission process, the latter being much more significant for 6 AU.

The picture provided by our calculations (both PCM-TD-DFT and CASPT2) is thus in qualitative agreement with the experimental trend, concerning both the steady-state absorption and fluorescence spectra as well as time-resolved experiments. On the other hand, some quantitative discrepancies can be found.

The ν_A of 6 AU is predicted to be blue-shifted by ~0.1 eV with respect to that of U, whereas the experimental absorption peak is red-shifted by 0.1 eV. In this respect, it is important to recall that the position of the maximum of an absorption band does not necessarily coincide with ν_A, since it depends also on the Franck−Condon factors between the ground and the excited states.[71,73] According to the considerations just reported, the $S\pi$ minima of 6 AU and U could exhibit different geometries and frequency shifts with respect to their S_0 minima, making a direct comparison between ν_A and the experimental absorption band difficult. In any case, for 6 AU the quantitative discrepancies between experiments and calculations are not larger than 0.2 eV, i.e., within the limit of the expected accuracy of PCM-TD-PBE0 calculations in solution.

A much larger difference, which cannot depend on the vibrational effect on the line shape, is instead found for 5 AU, whose calculated ν_A is red-shifted ~1 eV relative to those of 6 AU and U, while the difference between the experimental absorption peaks is smaller, ~0.5 eV. The similarity of the results provided by TD-PBE0, TD-CAM-B3LYP, and MS-CASPT2 calculations rules out that this discrepancy could be due to a partial $NH_2 \rightarrow$ ring charge transfer character of the $S_0 \rightarrow S\pi$ transition and to the well-known deficiency of standard functionals in describing CT transitions.[67] Actually, PCM/TD-PBE0 calculations show that the 5 AU ν_A is very sensitive to the presence of water molecules hydrogen bonded to the amino

group, i.e., when the nitrogen LP acts as a hydrogen bond acceptor. This result suggests that a very careful description of the first solvation shell of 5 AU, which is outside the scope of the present paper, eventually exploiting purposely tailored molecular dynamics simulation runs with a large number of water molecules, would be necessary to assess this topic. On the other hand, from the chemical−physical point of view, it is clear that "the degree of participation" of the nitrogen LP to the pyrimidine π system is one of the key factors modulating the ν_A in 5 AU. On one hand, it is thus possible that TD-DFT and MS-CASPT2 overestimate the delocalization of the nitrogen LP. On the other hand, 5 AU ν_A could be very sensitive to fine structural details, such as the exact NC_5 bond length, the degree of pyramidalization of the NH_2 group, or the so-called nitrogen umbrella motion. An accurate determination of such quantities not only would probably require a higher level theoretical treatment, but also, most of all, would call for the use of a suitable vibrational averaging procedure of the computed ν_A. In fact, preliminary calculations suggest that while small variation (∼0.07 Å) of the NC_5 bond length does not have a large impact on the computed ν_A (<0.1 eV), a strong pyramidalization of the amino group can be very influential, increasing the computed ν_A up to 0.4−0.5 eV.

5. Concluding Remarks

In this paper we have reported a detailed experimental and computational study of the absorption and fluorescence spectra of 5 AU and 6 AU, which are compared to those obtained for uracil. The presence of an amino substituent on the uracil C_5C_6 double bond has a dramatic effect on the absorption and the fluorescence spectra of U. Furthermore, 5 AU and 6 AU exhibit a very different behavior, indicating that their spectral features strongly depend on the position of the amino substituent. In fact, the lowest energy band of the steady-state absorption spectra of 5 AU is considerably red-shifted, noticeably less intense and broader than its counterpart in uracil. On the contrary, the 6 AU lowest energy absorption peak is close in energy to that of U, but it is much narrower and the transition is much more intense. The emission properties of the three compounds examined are also very different. 5 AU and, especially, 6 AU exhibit indeed a much larger Stokes shift as compared to U, and the emission peak of 5 AU is much narrower than that of 6 AU. These differences are mirrored by the very different dynamical behavior of the 5 AU and 6 AU bright excited state, 5 AU exhibiting much longer lifetimes than 6 AU and U.[58]

This puzzling behavior has been fully rationalized with the help of TD-DFT and MS-CASPT2 calculations. When the amino substituent is in position 5 of the pyrimidine ring, its LP has been shown to significantly interact with the HOMO of uracil in an antibonding way, explaining the very large red shift found in the lowest energy absorption band with respect to uracil. Such interaction is even stronger in the excited state, giving rise to a well-defined minimum on the Sπ surface, in line with a substantial Stokes shift found experimentally and to the much longer excited-state lifetime. Actually, the formation of a partial C_5N double bond could hinder the out-of-plane motion of the C5 substituent which, for U and its derivatives, is necessary to reach the CI between the bright excited and the ground state. As a consequence, we can expect that the deactivation mechanism result to be more complex than that found for U. Furthermore, the dark nπ* Sn state, which can take part into the Sπ dynamics in U and T, should not be involved in 5 AU, since it is significantly less stable than Sπ in the FC region.

For 6 AU, calculations indicate that on the Sπ surface a barrierless path connects the FC region with a CI with S_0, giving account for the short excited-state lifetime (<100 fs), like in the case of U.

The characteristics of the profile on the Sπ PES of the path connecting the FC region with the Sπ/S_0 CI, different for U, 5 AU, and 6 AU can explain some of the differences in the photophysics of these systems (see Figure 5). For 5 AU a steep path departing from planar geometries is followed by a plateau region, in which the system adopts a boat-like structure. For U, instead, our calculations indicate the presence of a planar plateau (although a very shallow nonplanar minimum is found, possibly not involved in the deactivation pathway), followed by a very steep "nonplanar" path toward the CI. For 6 AU, no minimum is found in this path. According to this picture, we can expect a much larger Stokes shift for 6 AU, since in this case most of the fluorescence should stem from the nonplanar region of the PES, for which S_0 is strongly destabilized; a significant but not so large Stokes shift is expected for 5 AU, due to the bent geometry of the Sπ minimum, quite different from the ground-state minimum, and a smaller Stokes shift is predicted for U due to the plateau found for planar geometries. Actually, experiments show that the Stokes shift of 6 AU ($\sim 14 \times 10^3$ cm^{-1}) is twice as large as that of U ($\sim 7 \times 10^3$ cm^{-1}) while for 5 AU an intermediate value ($\sim 12 \times 10^3$ cm^{-1}) is found.

Those considerations clearly highlight that a careful inspection of the steady-state spectra can provide fundamental information on the structure of the excited state and the presence of stationary and "quasi-stationary" points. For a bright transition, for example, very significant distortion of the FC geometry should be mirrored by a large Stokes shift. Analogously, the existence of intense red-energy tails could reveal the contribution of the portion of the PES more distant from the minima.

Our study also provides some interesting methodological hints, further supporting the reliability of TD-PBE0 calculations in the general description of the lowest energy excited states of nucleobases. In the gas phase, TD-DFT results in general agree satisfactorily with CASPT2 results, both reproducing qualitatively the trends found experimentally. An interesting point still open to analysis, but out of the scope of this paper, is the role of the mixing of lowest energy $\pi-\pi^*$ states on the topology of the Sπ PES, suggested by preliminary calculations with different computational methods (unpublished results). It has been shown that the lack of dynamic correlation might lead to an artificial mixing of two $\pi-\pi^*$ states of different natures (one of them statically neutral but dynamically ionic).[81,82] As a consequence, the agreement between the TD-DFT and MS-CASPT2 results for the Spi1 excited state is lower than for the rest of the states, given that Sπ1 is described by a mixed waefunction when the dynamical correlation is not properly taken into account.[83]

Concerning condensed phase calculations, state specific implementation of PCM/TD-DFT is confirmed to provide a very accurate description of static and dynamical solvent effects on the absorption and the emission spectra in solution, as shown by the remarkable agreement between the computed and the experimental Stokes shift. On the other hand, according to the analysis hereby reported, solute−solvent hydrogen bonds significantly modulate the spectroscopic properties of 5 AU and 6 AU, due to the hydrogen bonding ability of the amino substituent. Although a purposely tailored dynamical study should be necessary to assess the number and the coordination geometry of the water molecules of the first solvation shell, we

here show that simple models, based on chemical intuition, can provide very useful insights on the effect of explicit solute−solvent interactions.

On the balance, the results hereby reported provide another proof of the richness and the complexity of the microscopic mechanisms underlying the ultrafast decay of nucleobases. Nevertheless, thanks to the advances in the quantum mechanical methods, a direct comparison between experimental and computational results is possible for medium size molecules in their excited electronic states, also in the condensed phase, providing a fundamental tool for understanding processes of primary photophysical and photochemical interest.

Acknowledgment. The Spanish group is supported by DGSIC of the Ministerio de Ciencia e Innovación, Spain (Project No. CTQ2008-06644-C02-01/BQU) and by AGAUR of the Generalitat de Catalunya (Ajuts per potenciar els grups de recerca de qualitat, grant 2009SGR-462).

Supporting Information Available: R.I. thanks MIUR (PRIN 2008 and FIRB Futuro in Ricerca) for financial support. Vertical excitation energies of 5 AU, 6 AU, and of U computed in the gas phase at the TD-PBE0 level, in water solution at the PCM/TD-PBE0 level, and in water solution at the at the PCM/TD-CAM-B3LYP level. Graphical illustrations of the ground-state geometries optimized at the CASSCF(16,11)/6-32G* level for 5 AU·(H_2O), 5 AU with planar amino group, 5 AU with rotated amino group, and 6 AU·(H_2O). Cartesian coordinates of the S_0 minimum of 6 AU and 5 AU computed in aqueous solution at the PBE0/6-31+G(d,p) level. Cartesian coordinates of the S_0 minimum of 6 AU·7(H_2O) and 6 AU·8(H_2O) computed in aqueous solution at the PBE0/6-31G(d) level. Cartesian coordinates of the Sπ minimum of 5 AU computed in aqueous solution at the PBE0/6-31+G(d,p) level. Graphical illustrations of the calculation of band integrals of the 5 AU and 6 AU first absorption bands by lognorm-fitting on a wavenumber scale. Complete reference 77. This material is available free of charge via the Internet at http://pubs.acs.org.

References and Notes

(1) Crespo-Hernández, C. E.; Cohen, B.; Hare, P. M.; Kohler, B. *Chem. Rev.* **2004**, *104*, 1977.
(2) Middleton, C. T.; de La Harpe, K.; Su, C.; Law, Y. K.; Crespo-Hernandez, C. E.; Kohler, B. *Annu. Rev. Phys. Chem.* **2009**, *60*, 217.
(3) Markovitsi, D.; Gustavsson, T.; Talbot, F. *Photochem. Photobiol. Sci.* **2007**, *6*, 717.
(4) Markovitsi, D.; Gustavsson, T. Energy Flow in DNA Duplexes. In *Energy Transfer Dynamics in Biomaterial Systems*; Burghardt, I., May, V., Micha, D. A., Bittner, E. R., Eds.; Springer Verlag: Berlin, Heidelberg, 2009; Vol. 93, p 127.
(5) Markovitsi, D.; Gustavsson, T.; Banyasz, A. *Mutat. Res. Rev.* **2010**, *704*, 21.
(6) Gustavsson, T.; Improta, R.; Markovitsi, D. *J. Phys. Chem. Lett.* **2010**, *1*, 2025.
(7) Miller, D. L.; Weinstock, M. A. *J. Am. Acad. Dermatol.* **1994**, *30*, 774.
(8) Kraemer, K. H. *Proc. Natl. Acad. Sci. U.S.A.* **1997**, *94*, 11.
(9) Matsumura, Y.; Ananthaswamy, H. N. *Front. Biosci.* **2002**, *7*, D765.
(10) Markovitsi, D.; Talbot, F.; Gustavsson, T.; Onidas, D.; Lazzarotto, E.; Marguet, S. *Nature* **2006**, *441*, E7.
(11) Hare, P. M.; Crespo-Hernández, C. E.; Kohler, B. *Proc. Natl. Acad. Sci. U.S.A.* **2007**, *104*, 435.
(12) Hare, P. M.; Crespo-Hernández, C. E.; Kohler, B. *J. Phys. Chem. B* **2006**, *110*, 18641.
(13) Gustavsson, T.; Banyasz, A.; Lazzarotto, E.; Markovitsi, D.; Scalmani, G.; Frisch, M. J.; Barone, V.; Improta, R. *J. Am. Chem. Soc.* **2006**, *128*, 607.
(14) Gustavsson, T.; Sarkar, N.; Lazzarotto, E.; Markovitsi, D.; Barone, V.; Improta, R. *J. Phys. Chem. B* **2006**, *110*, 12843.
(15) Busker, M.; Nispel, M.; Haber, T.; Kleinermanns, K.; Etinski, M.; Fleig, T. *ChemPhysChem* **2008**, *9*, 1570.
(16) Gustavsson, T.; Sarkar, N.; Bányász, Á.; Markovitsi, D.; Improta, R. *Photochem. Photobiol.* **2007**, *83*, 595.
(17) Gustavsson, T.; Banyasz, A.; Sarkar, N.; Markovitsi, D.; Improta, R. *Chem. Phys.* **2008**, *350*, 186.
(18) Gustavsson, T.; Sarkar, N.; Lazzarotto, E.; Markovitsi, D.; Improta, R. *Chem. Phys. Lett.* **2006**, *429*, 551.
(19) Billinghurst, B. E.; Yeung, R.; Loppnow, G. R. *J. Phys. Chem. A* **2006**, *110*, 6185.
(20) Peticolas, W. R.; Rush, T., III. *J. Comput. Chem.* **1995**, *16*, 1261.
(21) Rush, T.; Peticolas, W. L. *J. Phys. Chem.* **1995**, *99*, 14647.
(22) Fodor, S. P. A.; Fava, R. P.; Hays, T. R.; Spiro, T. G. *J. Am. Chem. Soc.* **1985**, *107*, 1520.
(23) He, Y.; Wu, C.; Kong, W. *J. Phys. Chem. A* **2003**, *107*, 5145.
(24) He, Y.; Wu, C.; Kong, W. *J. Phys. Chem. A* **2004**, *108*, 943.
(25) Kang, H.; Lee, K. T.; Jung, B.; Ko, Y. J.; Kim, S. K. *J. Am. Chem. Soc.* **2002**, *124*, 12958.
(26) Ullrich, S.; Schultz, T.; Zgierski, M. Z.; Stolow, A. *Phys. Chem. Chem. Phys.* **2004**, *6*, 2796.
(27) Canuel, C.; Mons, M.; Piuzzi, F.; Tardivel, B.; Dimicoli, I.; Elhanine, M. *J. Chem. Phys.* **2005**, *122*, 074316.
(28) Karunakaran, V.; Kleinermanns, K.; Improta, R.; Kovalenko, S. A. *J. Am. Chem. Soc.* **2009**, *131*, 5839.
(29) Lorentzon, J.; Fülscher, M. P.; Roos, B. O. *J. Am. Chem. Soc.* **1995**, *117*, 9265.
(30) Matsika, S. *J. Phys. Chem. A* **2004**, *108*, 7584.
(31) Perun, S.; Sobolewski, A. L.; Domcke, W. *J. Phys. Chem. A* **2006**, *110*, 13238.
(32) Merchán, M.; Gonzalez-Luque, R.; Climent, T.; Serrano-Andres, L.; Rodriguez, E.; Reguero, M.; Pelaez, D. *J. Phys. Chem. B* **2006**, *110*, 26471.
(33) Climent, T.; Gonzalez-Luque, R.; Merchán, M.; Serrano-Andres, L. *Chem. Phys. Lett.* **2007**, *441*, 327.
(34) Santoro, F.; Barone, V.; Gustavsson, T.; Improta, R. *J. Am. Chem. Soc.* **2006**, *128*, 16312.
(35) Hudock, H. R.; Levine, B. G.; Thompson, A. L.; Satzger, H.; Townsend, D.; Gador, N.; Ullrich, S.; Stolow, A.; Martinez, T. J. *J. Phys. Chem. A* **2007**, *111*, 8500.
(36) Zechmann, G.; Barbatti, M. *J. Phys. Chem. A* **2008**, *112*, 8273.
(37) Szymczak, J. J.; Barbatti, M.; Hoo, J. T. S.; Adkins, J. A.; Windus, T. L.; Nachtigallova, D.; Lischka, H. *J. Phys. Chem. A* **2009**, *113*, 12686.
(38) Lan, Z. G.; Fabiano, E.; Thiel, W. *J. Phys. Chem. B* **2009**, *113*, 3548.
(39) Epifanovsky, E.; Kowalski, K.; Fan, P. D.; Valiev, M.; Matsika, S.; Krylov, A. I. *J. Phys. Chem. A* **2008**, *112*, 9983.
(40) Yoshikawa, A.; Matsika, S. *Chem. Phys.* **2008**, *347*, 393.
(41) Ludwig, V.; Coutinho, K.; Canuto, S. *Phys. Chem. Chem. Phys.* **2007**, *9*, 4907.
(42) Zazza, C.; Amadei, A.; Sanna, N.; Grandi, A.; Chillemi, G.; Di Nola, A.; D'Abramo, M.; Aschi, M. *Phys. Chem. Chem. Phys.* **2006**, *8*, 1385.
(43) Improta, R.; Barone, V. *J. Am. Chem. Soc.* **2004**, *126*, 14320.
(44) Improta, R.; Barone, V. *Theor. Chem. Acc.* **2008**, *120*, 491.
(45) Mercier, Y.; Santoro, F.; Reguero, M.; Improta, R. *J. Phys. Chem. B* **2008**, *112*, 10769.
(46) Improta, R.; Barone, V.; Lami, A.; Santoro, F. *J. Phys. Chem. B* **2009**, *113*, 14491.
(47) Ismail, N.; Blancafort, L.; Olivucci, M.; Kohler, B.; Robb, M. A. *J. Am. Chem. Soc.* **2002**, *124*, 6818.
(48) Merchán, M.; Serrano-Andrés, L.; Robb, M. A.; Blancafort, L. *J. Am. Chem. Soc.* **2005**, *127*, 1820.
(49) Hudock, H. R.; Martinez, T. J. *ChemPhysChem* **2008**, *9*, 2486.
(50) Zgierski, M. Z.; Patchkovskii, S.; Fujiwara, T.; Lim, E. C. *J. Phys. Chem. A* **2005**, *109*, 9384.
(51) Improta, R. *Phys. Chem. Chem. Phys.* **2008**, *10*, 2656.
(52) Santoro, F.; Barone, V.; Improta, R. *Proc. Natl. Acad. Sci. U.S.A.* **2007**, *104*, 9931.
(53) Serrano-Andres, L.; Merchán, M.; Borin, A. C. *Proc. Natl. Acad. Sci. U.S.A.* **2006**, *103*, 8691.
(54) Serrano-Andres, L.; Merchán, M.; Borin, A. C. *Chem.−Eur. J.* **2006**, *12*, 6559.
(55) Serrano-Andres, L.; Merchán, M.; Borin, A. C. *J. Am. Chem. Soc.* **2008**, *130*, 2473.
(56) Improta, R.; Santoro, F.; Barone, V.; Lami, A. *J. Phys. Chem. A* **2009**, *113*, 15346.
(57) Santoro, F.; Barone, V.; Improta, R. *J. Am. Chem. Soc.* **2009**, *131*, 15232.
(58) Bányász, Á.; Gustavsson, T.; Keszei, E.; Improta, R.; Markovitsi, D. *Photochem. Photobiol. Sci.* **2008**, *7*, 765.
(59) Miertus, S.; Scrocco, E.; Tomasi, J. *Chem. Phys.* **1981**, *55*, 117.
(60) Tomasi, J.; Mennucci, B.; Cammi, R. *Chem. Rev.* **2005**, *105*, 2999.
(61) Scalmani, G.; Frisch, M. J.; Mennucci, B.; Tomasi, J.; Cammi, R.; Barone, V. *J. Chem. Phys.* **2006**, *124*, 094107.

(62) Improta, R.; Barone, V.; Scalmani, G.; Frisch, M. J. *J. Chem. Phys.* **2006**, *125*, 054103.
(63) Improta, R.; Scalmani, G.; Frisch, M. J.; Barone, V. *J. Chem. Phys.* **2007**, *127*, 074504.
(64) Adamo, C.; Barone, V. *J. Chem. Phys.* **1999**, *110*, 6158.
(65) Ernzerhof, M.; Scuseria, G. E. *J. Chem. Phys.* **1999**, *111*, 911.
(66) Adamo, C.; Scuseria, G. E.; Barone, V. *J. Chem. Phys.* **1999**, *111*, 2889.
(67) Dreuw, A.; Head-Gordon, M. *Chem. Rev.* **2005**, *105*, 4009.
(68) Burke, K.; Werschnik, J.; Gross, E. K. U. *J. Chem. Phys.* **2005**, *123*, 062206.
(69) Yanai, T.; Tew, D. P.; Handy, N. C. *Chem. Phys. Lett.* **2004**, *393*, 51.
(70) Tawada, Y.; Tsuneda, T.; Yanagisawa, S.; Yanai, T.; Hirao, K. *J. Chem. Phys.* **2004**, *120*, 8425.
(71) Barone, V.; Improta, R.; Rega, N. *Acc. Chem. Res.* **2008**, *41*, 605.
(72) Improta, R.; Barone, V.; Santoro, F. *Angew. Chem.-Int. Edit.* **2007**, *46*, 405.
(73) Santoro, F.; Improta, R.; Lami, A.; Bloino, J.; Barone, V. *J. Chem. Phys.* **2007**, *126*, 084509.
(74) Barone, F.; Bonincontro, A.; Mazzei, F.; Minoprio, A.; Pedone, F. *Photochem. Photobiol.* **1995**, *61*, 61.
(75) Improta, R.; Barone, V.; Santoro, F. *J. Phys. Chem. B* **2007**, *111*, 14080.
(76) Jimenez, R.; Fleming, G. R.; Kumar, P. V.; Maroncelli, M. *Nature* **1994**, *369*, 471.
(77) Frisch, M. J.; *Gaussian Development Version*, Revision F.02; Gaussian, Inc.: Wallingford, CT, 2007.
(78) Bearpark, M. J.; Robb, M. A.; Schlegel, H. B. *Chem. Phys. Lett.* **1994**, *223*, 269.
(79) Karlstrom, G.; et al. *Comput. Mater. Sci.* **2003**, *28*, 222.
(80) Onidas, D.; Markovitsi, D.; Marguet, S.; Sharonov, A.; Gustavsson, T. *J. Phys. Chem. B* **2002**, *106*, 11367.
(81) Angeli, C. *J. Comput. Chem.* **2009**, *30*, 1319.
(82) Angeli, C. *Int. J. Quantum Chem.* **2010**, *110*, 2436.
(83) Angeli, C.; Improta, R.; Santoro, F. *J. Chem. Phys.* **2009**, *130*, 174307.

JP105267Q